

# An All-Solid-State Polymeric Membrane chloride ion-selective Electrode with Nanowires poly(3,4-ethylenedioxythiophene) as Solid Contact

Zhe Li<sup>1</sup>, Ming Lei<sup>2,3</sup>, Juan Chen<sup>1,\*</sup>, Xin Qi<sup>2,3</sup>

<sup>1</sup> College of Information Science and Technology, Beijing University of Chemical Technology, Beijing 100029, PR China

<sup>2</sup> College of Science, Beijing University of Chemical Technology, Beijing 100029, PR China

<sup>3</sup> Beijing Key Laboratory of Environmentally Harmful Chemical Analysis, Beijing 100029, PR China

\*E-mail: [jchen@mail.buct.edu.cn](mailto:jchen@mail.buct.edu.cn)

*Received:* 21 July 2017 / *Accepted:* 21 September 2017 / *Published:* 12 November 2017

---

This paper reports the development of a novel all-solid-state polymeric membrane Cl<sup>-</sup>-selective electrode, based on nanowires poly(3,4-ethylenedioxythiophene) (PEDOT) as solid contact. The nanowires PEDOT films are synthesized on the glassy carbon electrode surface by electrochemical galvanostatic method in the cetyltrimethylammonium bromide aqueous solution. The electrochemical performances of nanowires PEDOT films are evaluated by cyclic voltammetry and electrochemical impedance spectroscopy, which indicate that the nanowires PEDOT have large redox capacitance and fast charge-transfer rate. This makes the PEDOT films suitable for solid contact layer of all-solid-state ion selective electrode. With the nanowires PEDOT, the all-solid-state Cl<sup>-</sup>-selective electrode shows a Nernstian response in the range from  $1.0 \times 10^{-4}$  to  $1.0 \times 10^{-1}$  M, and the detection limit is  $1.0 \times 10^{-5}$  M. The experiment results of potentiometric measurements and chronopotentiometry suggest that the electrode potential is very stable and the potential drift is significantly decreased.

---

**Keywords:** Chloride quantification, Electrochemistry, Poly(3,4-ethylenedioxythiophene), Sensor, Solid contact

## 1. INTRODUCTION

There is a strong demand of measuring the concentration of chloride ions in many areas, such as biomedical and clinical analysis [1,2], environmental monitoring [3,4], industrial and process control [5,6], and some others. Compare with fluorescent method [7,8], ion chromatography [9] and laser-induced breakdown spectroscopy [10], electrode method have a significant advantage because of their small size, portability, energy saving and inexpensive features [11,12]. For example, Jui-Fu Cheng et al. fabricated a chloride ion sensor based on indium tin oxide glass with polymeric membrane

[13]. Cheanyeh Cheng et al. synthesized a new sensor membrane based on copolymeric ion-exchanger resin and ionophore for the detection of chloride ion [1]. Jung-Chuan Chou et al. fabricated a polymeric membrane array chlorine ion sensor integrated on microfluidic device for measuring concentration of the chloride ion [14].

In recent years, all-solid-state ion select electrodes (ISEs) have attracted a lot of attention. Different from traditional liquid contact ISEs, all-solid-state ISEs are more convenient to use and easy to maintenance [15,16]. But the potential of all-solid-state ISEs is not stable enough since the electron transfer process is hindered from ion selective membrane to conductor electrode [17]. To resolve the problem, conducting polymers, such as polypyrrole, poly(3-octylthiophene), polyaniline and poly(3,4-ethylene-dioxythiophene) (PEDOT), are often used as solid contact layer of the all-solid-state ISEs, and the potential response of the solid contact ISEs are more stable than traditional all-solid-state ISEs. [17]. Furthermore, the performance of those solid contact materials were reinforced by microstructure adjustment or doping modification. For instance, Lobna. A. Hussein et al. found that polyaniline nanoparticles had a better ion-to-electron performance than polyaniline microparticles [18]. Zaneta Pławinska et al. found the electrodes with PEDOT doped by chloride anions and chloride ion-selective membrane obtained a much smaller capacitance limitation than PEDOT(PSS) electrode [19].

A few years ago, Yu Li, Bichen Wang et al. found a way to synthesize nanowires PEDOT. The nanowires (nanorods) PEDOT are synthesized on tantalum by galvanostatic electrochemical polymerization technology in cetyltrimethylammonium bromide (CTAB) aqueous solution. Different from hard-template polymerization [20,21], soft-template polymerization is more suitable for synthesizing the conducting polymer on glassy carbon (GC) electrode because the template is easy to remove. The CTAB is used both as the supporting salt and the surfactant. Also, the CTAB is the soft-template [22,23]. The structure of PEDOT can be influenced by the CTAB concentration, hydron concentration, current density and polymerization temperature. When the concentration of CTAB is about 0.01 M, the 3,4-ethylene-dioxythiophene (EDOT) and CTAB can produce a special wirelike shape. The EDOT monomers are coated by CTAB except the both ends. One of this ends sticks to the surface of electrode, while PEDOT grows from another end [24]. Therefore, the nanowires PEDOT had two features of large surface area and chloride anions doping, which may improve the stability and performance of the all-solid-state chloride ion-selective electrodes. However, the chloride ion-selective electrodes base on this material has not been reported.

In this work, we use the nanowires PEDOT as solid contacts to fabricate an all-solid-state chloride ion-selective electrodes. The nanowires PEDOT film was synthesized on a GC electrode by electrochemical galvanostatic method. In order to evaluate the performance, the Cl<sup>-</sup>-ISEs were tested by cyclic voltammetry, chronopotentiometry and electrochemical impedance spectroscopy. The potentiometric performance and selectivity were also investigated.

## **2. MATERIALS AND EXPERIMENTAL**

### *2.1. Materials*

The monomer EDOT (>99%), Poly (vinyl chloride) (PVC) of high molecular weight, 3,6-didodecyloxy-4,5-dimethyl-o-phenylene-bis(mercury chloride) (chloride ionophore III; ETH9033),

tridodecylmethylammonium chloride were obtained from Sigma-Aldrich. NaCl (99.95-100.05%; datum chemical reagents) was obtained from Beijing Chemical Works. CTAB was obtained from Tokyo Chemical Industry Co. Ltd. tetrahydrofuran (THF), bis(2-ethylhexyl)sebacate (DOS) and other materials were obtained from Sinopharm Chemical Reagent and were analytical-reagent grade. Dionized water (resistivity = 18.2 M $\Omega$ cm) was obtained with Millipore (ADVANTAGE A10) ultrapure water system.

## 2.2. Instrument and equipment

The constant temperature bath was provided by Thermo Fisher Scientific (HAAKE SC100-A10). Unless otherwise specified, all the electrochemical experiments were performed at 25 °C.

The potentiometric performance test were performed with a high resolution digital voltmeter (Agilent 34401A) connected to a computer for data acquisition via a GPIB card (Agilent 82357B). The reference electrode was an Ag/AgCl double junction electrode with 3 M KCl in the first salt bridge and 0.1 M K<sub>2</sub>SO<sub>4</sub> in the second salt bridge. During experimentation, all liquid junction potentials were corrected by Henderson equation, and activity coefficients were calculated by using the Debye–Hückel equation.

Cyclic voltammetry was performed using a CHI 660E electrochemical workstation (Shanghai Chenhua Apparatus Corporation). Cyclic voltammetry was measured in a conventional three-electrode cell where the chloride electrode was connected as the working electrode and the electrolyte is 0.1 M KCl aqueous solution. The reference electrode was an Ag/AgCl (3 M KCl) double junction electrode and the auxiliary electrode was a platinum wire. The Cyclic voltammetry measurements were performed at a fixed potential range from -0.5 V to +0.5 V with a scan rate of 100 mVs<sup>-1</sup>.

Electrochemical impedance spectroscopy was measured in a three-electrode cell just as it was in cyclic voltammetry measurement. The measurement was performed in the frequency range of 20 mHz-10 KHz by using a sine wave signal with a peak-to-peak voltage amplitude of 10 mV.

Chronopotentiometric measurements were performed in 0.1 M KCl aqueous solution with a constant current of + 1 nA for the first 60 s and - 1 nA for the next 60 s.

High-resolution scanning electron microscope (Hitachi SU8010) was used for the morphology consideration.

## 2.3. Electrode preparation

### 2.3.1. Electrochemical polymerization of PEDOT

A conventional three-electrode cell was used for PEDOT electrochemical polymerization. The working electrode was a GC disk with 0.07 cm<sup>2</sup> effective area. The reference electrode was an Ag/AgCl (3M KCl) double junction electrode and the auxiliary electrode was a platinum wire. Before the experiment, all GC electrode should polish with 0.05  $\mu$ m Al<sub>2</sub>O<sub>3</sub> powder and rinse in water, acetone and water step by step. The aqueous solution containing 0.01 M CTAB, 0.01 M EDOT and 0.1 M HCl was prepared and stored in 0 °C. PEDOT films grew on the surface of GC electrode in the prepared

solutions. A constant current of 0.0707 mA ( $1 \text{ mA/cm}^2$ ) was applied for 1414 s to polymerization charge of 100 mC. After polymerization, the electrode were cleaned by acetone and deionized water to remove the template. For comparison, a constant current of 0.03535 mA was applied on another electrode for 2828 s to polymerization charge of 100 mC. The above-prepared electrodes are named as GC/PEDOT (I) and GC/PEDOT (II) electrode, respectively.

### 2.3.2. Fabrication of $\text{Cl}^-$ -selective electrode

The polymer membrane components including chloride ionophore III (1.0 wt.%), tridodecylmethylammonium chloride (0.2 wt.%), PVC (33 wt.%) and DOS (65.8 wt.%). All components were dissolved in THF (dry mass= 13.65%). All-solid-state  $\text{Cl}^-$ -ISEs were prepared by drop-casting 20  $\mu\text{L}$  of the membrane solution on the surface of the PEDOT, and then stored vertical for over 24 h until it completely dry. For comparison, the membrane solution also drop-casting 20 $\mu\text{L}$  on a bare GC electrode. This electrode is named as GC/ $\text{Cl}^-$ -ISE. The electrodes were conditioning in 0.1 M KCl solution for 1 day before experiment. When not in use, the electrodes were stored in 0.1M KCl solution.

## 3. RESULT AND DISCUSSION

### 3.1. Characterization of the PEDOT film

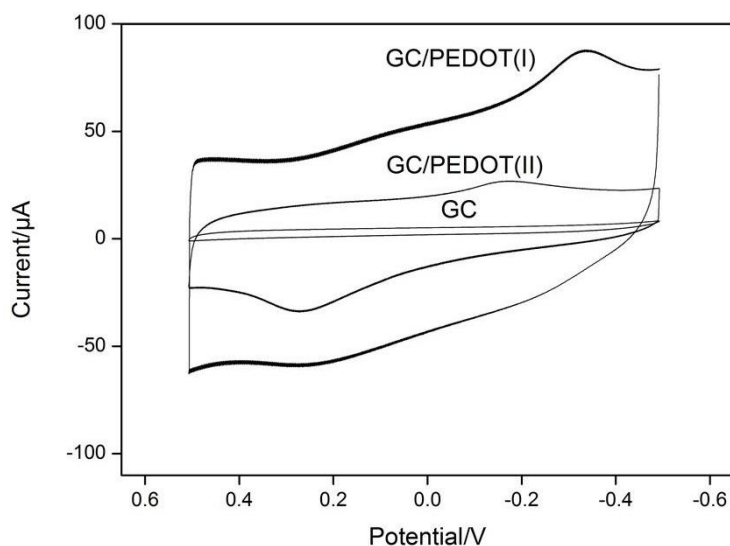


**Figure 1.** Cyclic voltammetry for the GC, GC/PEDOT (I) and GC/PEDOT (II) electrodes in 0.1 M KCl solution with a scan rate of 100 mV/s.

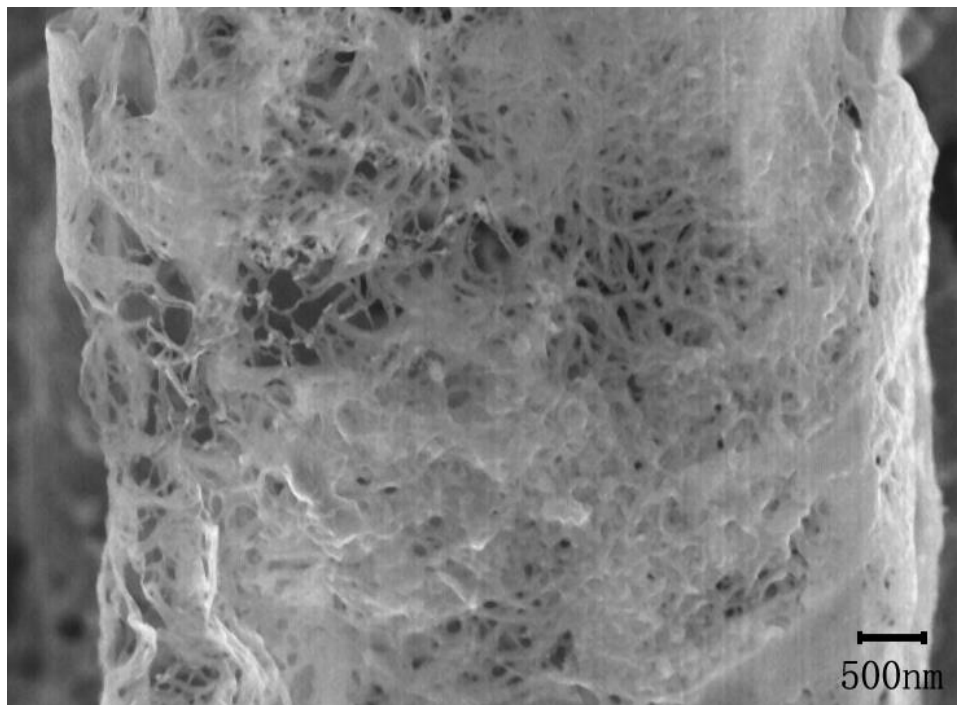


**Figure 2.** SEM images of PEDOT (I) electrode.

The nanowires PEDOT was electrochemically polymerized on the GC surface by electrochemical galvanostatic method [25,26]. With different current density, the PEDOT grew into different morphologies. When the current density is  $1 \text{ mA/cm}^2$ , the PEDOT formed a wirelike microstructure. When the current density is  $0.5 \text{ mA/cm}^2$ , the PEDOT formed a random microstructure because EDOT monomers only can be initiated to polymerize from the limited active nucleus [24].

The electrochemical properties of the GC, GC/PEDOT (I) and GC/PEDOT (II) electrodes were analysed in  $0.1 \text{ M KCl}$  solution by cyclic voltammetry (3rd cycle). As shown in Fig.1, the curve of the bare GC electrode is similar to a straight line and the capacitive current of this electrode is significantly less than other two electrodes, while the GC/PEDOT (I) electrode has the largest capacitive current. The 1 dimension nanowires structure can not only provide higher specific surface area than flat surface morphology, but also decrease the diffusion distances for ion exchange or ion transport, which may enhance the contact from the ionic solution to the active sites of the conducting film [24], increase the capacitor capacity and improve the charge/discharge performance [27]. Since the cyclic voltammetry curve of GC/PEDOT (I) electrode are similar to ideal capacitor, and the nanowires structure PEDOT have the largest redox capacitance, the PEDOT (I) is best suited for contact layer.

SEM image of the PEDOT (I) is shown in Fig.2. The PEDOT nanowires were highly curved and intertwined, several microns long, but only about 50 nanometers in diameter. In addition, those nanowires PEDOT finally formed microrods PEDOT with 3-5 nanometers in diameter on the surface of GC electrode.

3.2. Potentiometric measurements

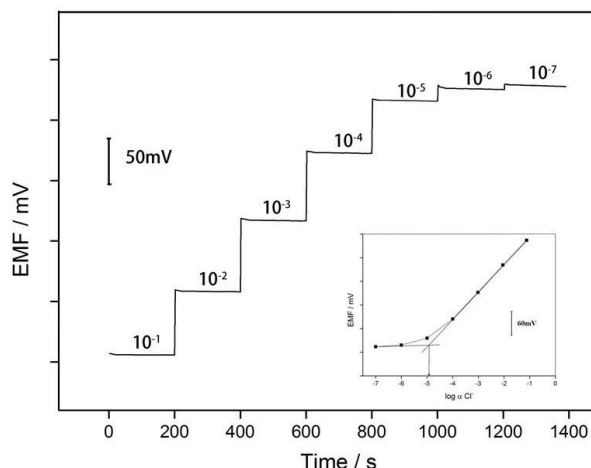


**Figure 3.** Electrode potential changes with time in NaCl solution in the concentration range from  $1.0 \times 10^{-1}$  to  $1.0 \times 10^{-7}$  M. The inset shows the calibration curve of GC/PEDOT (I)/Cl<sup>-</sup>-ISE.

The potentiometric measurements of GC/PEDOT (I)/Cl<sup>-</sup>-ISE was done in NaCl solution at the concentration range from  $1.0 \times 10^{-1}$  to  $1.0 \times 10^{-7}$  M. As shown in Fig.3, each concentration was tested for 200 s and the electrode potential rose with solution concentration decreased. The linear range is from  $1.0 \times 10^{-1}$  to  $1.0 \times 10^{-4}$  M with a slop close to Nernstian slope ( $-58.1 \pm 1.5$  mV/log<sub>a</sub>c<sub>Cl</sub>, n=4, R<sup>2</sup>=0.99987). When the concentration blow  $1.0 \times 10^{-4}$  M, the slope turned to nonlinearity. The calculated results by finding intersection between two slope line show that the limit of detection of the electrode is  $1.0 \times 10^{-5}$  M.

**Table 1.** Comparison of polymeric membrane chloride ion-selective electrodes (ETH9033 as ionophore).

Electrode	Slope (mV/decade)	Linear range (M)	Detection limit (M)	Linearity (R2)	Reference
Liquid filled electrode #1	56.9mV	$10^{-5} - 10^{-1}$	$1 \times 10^{-5}$	-	[11]
Indium Tin Oxide Glass electrode	54.0mV	$10^{-4} - 10^{-1}$	$8 \times 10^{-5}$	0.990	[13]
Liquid filled electrode #2	59.2mV	$10^{-4} - 10^{-2}$	$6.9 \times 10^{-5}$	0.993	[1]
Microfluidic sensor	33.7mV	$10^{-4} - 10^{-1}$	-	0.996	[14]
Solid contact electrode	58.1mV	$10^{-4} - 10^{-1}$	$1 \times 10^{-5}$	0.999	This work

Compare with other polymeric membrane chloride ion-selective electrodes(ETH9033 as ionophore), as shown in the Table 1, the most parameters of GC/PEDOT (I)/Cl<sup>-</sup>-ISE (Solid contact

electrode) is close to the liquid filled electrode, and the linearity of the GC/PEDOT (I)/Cl<sup>-</sup>-ISE is superior than other reported chloride ion-selective electrodes. This proved that the nanowires PEDOT can effectively improve the potentiometric performance of the chloride ion-selective electrode.

### 3.3. Selectivity

The selectivity coefficients of the GC/Cl<sup>-</sup>-ISE, GC/PEDOT (I)/Cl<sup>-</sup>-ISE and GC/PEDOT (II)/Cl<sup>-</sup>-ISE were determined by the separate solution method [28]. As shown in the Table 2, the numerical values of those three electrode are close to each other, which indicate that nanowires PEDOT have negligible impact on selectivity of the electrode. Compare with literature [29], the selectivity of the ISEs had improved considerably with the help of chloride ionophore III. On the other hand, literature [11] showed a better selectivity than our ISEs, this probably because the ratio of membrane component is different, and the selectivity coefficients is mainly depend on the membrane but not the solid contact layer. Similar to Julia Szucs et al. results [30], nanostructured solid contact layer has little influence on selectivity of all-solid-states membrane ISEs.

**Table 2.** Logarithmic selectivity coefficients ( $\log K_{Cl,j}$ ) for GC/PEDOT (I)/Cl<sup>-</sup>-ISE, GC/PEDOT (II)/Cl<sup>-</sup>-ISE and GC/Cl<sup>-</sup>-ISE. All selectivities were determined by the separate solution method at 25°C.

Anion	GC/PEDOT (I)/ Cl <sup>-</sup> -ISE	GC/PEDOT (II)/ Cl <sup>-</sup> -ISE	GC/Cl <sup>-</sup> -ISE	Literature [16]	Literature [1]
I <sup>-</sup>	3.9	3.9	3.7	-[a]	-0.7
Br <sup>-</sup>	0.8	0.8	0.8	1.6	-0.7
Salicylat e <sup>-</sup>	0.9	0.8	0.8	3.2	-0.8
ClO <sub>4</sub> <sup>-</sup>	1.6	1.5	1.4	4.3	-0.2
NO <sub>3</sub> <sup>-</sup>	-0.8	-0.9	-0.9	2.0	-2.5
Acetate <sup>-</sup>	-3.9	-3.9	-4.0	-[a]	-5.2
F <sup>-</sup>	-2.6	-2.6	-2.7	-2.2	-5.2
HCO <sub>3</sub> <sup>-</sup>	-4.5	-4.5	-4.6	-1.2	-4.7
HPO <sub>4</sub> <sup>2-</sup>	-3.6	-3.7	-3.8	-[a]	-5.2
SO <sub>4</sub> <sup>2-</sup>	-3.3	-3.3	-3.2	-2.5	-5.5

[a] Not test in the literature.

### 3.4. Chronopotentiometry

Chronopotentiometry is an effective way to investigate the electrical capacity of the PEDOT film and the potentiometric stability of the electrodes. A current of  $\pm 1$  nA were applied to the working electrode and the electrode potential was recorded, as shown in Fig.4. The potential drift ( $\Delta E/\Delta t$ ) of GC/PEDOT (I)/Cl<sup>-</sup>-ISE is  $6.2 \mu\text{Vs}^{-1}$ , which is far below GC/Cl<sup>-</sup>-ISE ( $419.1 \mu\text{Vs}^{-1}$ ). The low-frequency capacitance ( $C_L$ ) can be calculated as [31]:

$$\text{Potential drift} = \Delta E/\Delta t = i/C_L \quad (3-1)$$

The low-frequency capacitance of GC/PEDOT (I)/Cl<sup>-</sup>-ISE is 161 μF, which is much larger than GC/Cl<sup>-</sup>-ISE (2.39 μF). Table 3 shows some solid contact materials tested by chronopotentiometry with 1nA current, which suggest nanowires PEDOT have a relatively slow potential drift and a comparatively large capacitance. Those results indicate that the potential stability of the electrode is significantly improved by using the PEDOT (I) film studied (polymerization current density 1 mA/cm<sup>2</sup>) as solid contact layer.

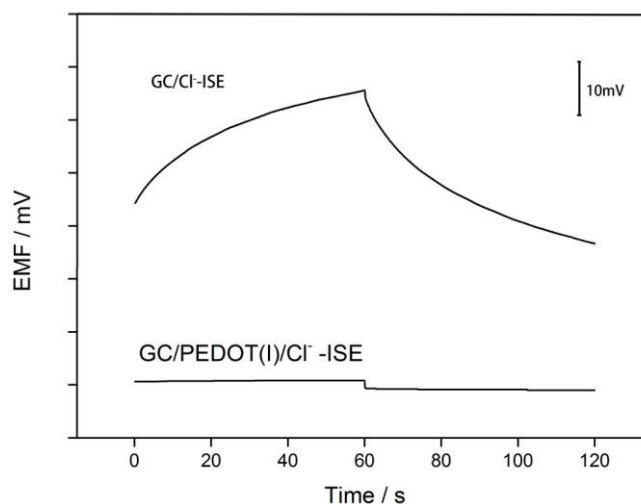


**Figure 4.** Chronopotentiometry for GC/PEDOT (I)/Cl<sup>-</sup>-ISE and GC/Cl<sup>-</sup>-ISE in a 0.1 M KCl aqueous solution.

**Table 3.** Potential drifts and low-frequency capacitance of all-solid state ISEs.

Solid contact	Potential drift (μV/s)	Capacitance (μF)	Reference
TCNQ	6.5	154	[32]
Gold nanoclusters	8.5	118	[33]
TTF	16.5	61	[34]
Graphene	12.8	78	[35]
Carbon nanotubes	17.0	60	[36]
PEDOT nanowires	6.2	161	This work

### 3.5. Impedance measurement

The impedance spectrum of GC/PEDOT (I) electrode without ion select membrane was investigated in 0.1M KCl solution. As shown in Fig.5, the impedance spectrum of GC/PEDOT (I) electrode is a vertical line which had a slight deviation in high frequency region. The redox capacitance ( $C_{LF}$ ) can be calculated as [37]:

$$C_{LF} = 1/(2\pi fZ'' ) \tag{3-2}$$

Where  $f$  is the lowest frequency of the spectra (0.02Hz), and  $Z''$  is the imaginary part at this frequency. The  $C_{LF}$  of GC/PEDOT (I) electrode and GC electrode is 142μF and 14.4μF, respectively, which indicate the redox capacitance was significantly enhanced by the nanowires PEDOT. Fig.6 present

EIS Nyquist plots of those GC/C<sup>-</sup>-ISE and GC/PEDOT (I)/Cl<sup>-</sup>-ISE electrodes in KCl solution. Both GC/PEDOT (I)/Cl<sup>-</sup>-ISE and GC/Cl<sup>-</sup>-ISE show a obvious semicircle in the high frequency range, but the radius of GC/PEDOT (I)/Cl<sup>-</sup>-ISE is much smaller than GC/Cl<sup>-</sup>-ISE. With nanowires PEDOT film, the bluk membrane resistance drop from 2.1 MΩ to 1.4 MΩ, which indicate the contact resistance between GC and membrane can be facilitated by the nanowires PEDOT film with a large specific surface area. Between the GC and ion-selective membrane, a small redox capacitance with a large charge-transfer resistance connected in parallel, makes the GC /Cl<sup>-</sup>-ISE shows a large low frequency semicircle [38], the charge-transfer resistance (calculate by ZsimpWin software) is 26.7MΩ. For GC/PEDOT (I)/Cl<sup>-</sup>-ISE, the low frequency branch is much more closer to real impedance axis [31], and the curvature is unconspicuous, the chage-transfer resistance fall to 1.1MΩ. This result indictae the charge-transfer resistance can be improved by the solid contact of nanowires PEDOT.

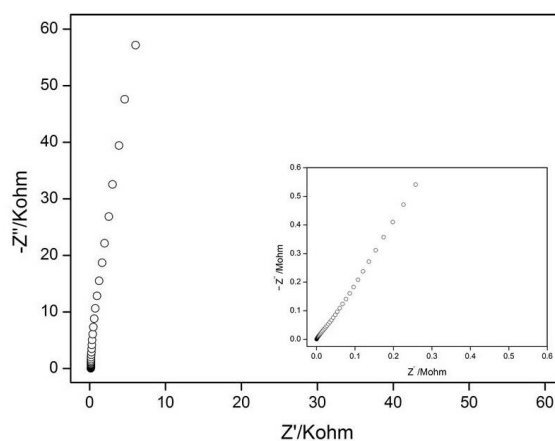


**Figure 5.** Impedance spectra of GC/PEDOT (I) electrode. The frequency range is 20 mHz-10 KHz and the amplitude is 5 mV. The inset image is the impedance spectra of GC electrode.

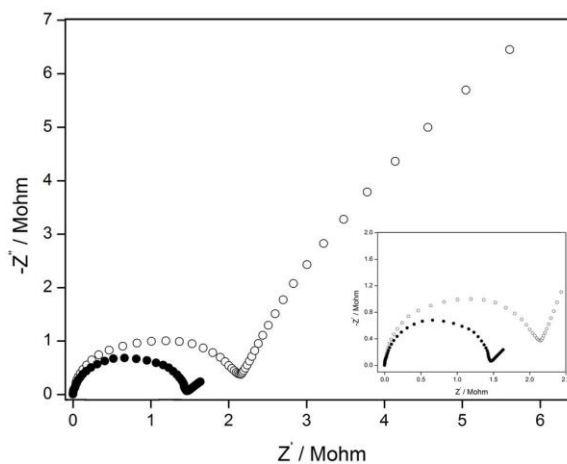


**Figure 6.** Impedance spectra of GC/PEDOT (I)/Cl<sup>-</sup>-ISE (solid circle) and GC/Cl<sup>-</sup>-ISE (hollow circle) recorded in 0.1M KCl. The frequency range is 20 mHz-10 KHz and the amplitude is 10 mV. The inset image is the magnification of the impedance spectra.

### 3.6. Water layer test

The potentiometric stability of GC/PEDOT (I)/Cl<sup>-</sup>-ISE and GC/Cl<sup>-</sup>-ISE was investigated in 0.1 M Na<sub>2</sub>SO<sub>4</sub>, 0.1M KCl and 0.1 M Na<sub>2</sub>SO<sub>4</sub> solution, respectively. As shown in Fig.7, there were no significant different between two electrodes in the first 1.5 h. Once the electrode moved into 0.1 M NaCl solution, the potential of GC/Cl<sup>-</sup>-ISE showed a negative drift, while the GC/PEDOT (I)/Cl<sup>-</sup>-ISE is much lower. This result indicate that the water layer can effectively be reduced by nanowires PEDOT.

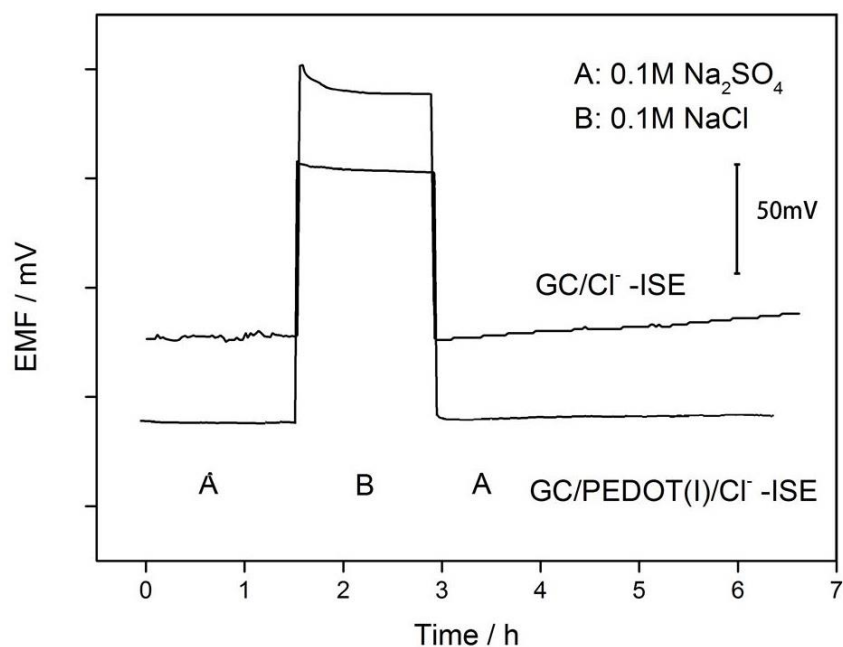


**Figure 7.** Water layer tests for GC/PEDOT (I)/Cl<sup>-</sup>-ISE and GC/Cl<sup>-</sup>-ISE in 0.1 M Na<sub>2</sub>SO<sub>4</sub> (A) and 0.1 M NaCl (B).

### 3.7. Sensitivity to O<sub>2</sub>, CO<sub>2</sub> and light

Sensitivity of the GC/PEDOT (I)/Cl<sup>-</sup>-ISE to O<sub>2</sub>, CO<sub>2</sub> and room light was investigated in 0.1M KCl solution. The gas sensitivity test cycles every 0.5 h. Before and after the experiment, N<sub>2</sub> was bubbling into the solution to remove O<sub>2</sub>, CO<sub>2</sub> or other interfering gas. As shown in Fig.8, GC/PEDOT (I)/Cl<sup>-</sup>-ISE is only slightly sensitive to O<sub>2</sub>, and almost insensitivity to CO<sub>2</sub>. The photosensitive test of GC/PEDOT (I)/Cl<sup>-</sup>-ISE was also studied by alternated turning on and off the filament lamp. From Fig. 8, there has no obvious difference between two lighting environment, which proved that the GC/PEDOT (I)/Cl<sup>-</sup>-ISE has a good potential stability under the room light.

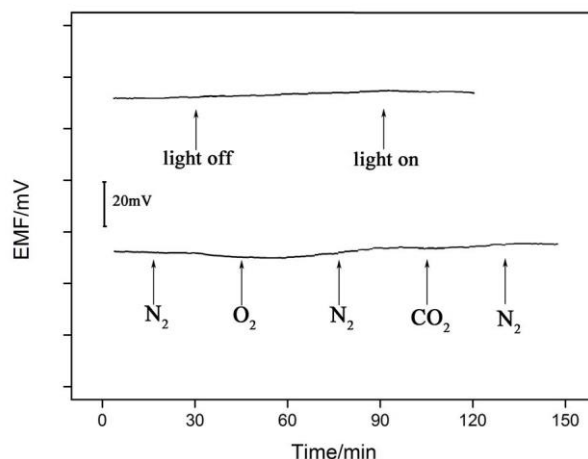


**Figure 8.** Sensitivity to  $O_2$ ,  $CO_2$  and room light in 0.1 M KCl solution for GC/PEDOT (I)/ $Cl^-$ -ISE.

### 3.8. Real Sample analysis

To evaluate the real performance of the GC/PEDOT (I)/ $Cl^-$ -ISE, a real sample test was carried out. The water sample was collected from the inlet of industrial boiler, and stored in a closed container before the test. After that, NaCl was added into different volumetric flask and dissolved in the water sample. As shown in the Table 4, the recoveries of results were from 97.8% to 98.6%, which indicated that the GC/PEDOT (I)/ $Cl^-$ -ISE was both sensitive and stable enough for real water analysis.

**Table 4.** Determination of  $Cl^-$  in real samples.

Samples	Added (mM)	Expected (mM)	Found (mM)	Recovery (%)
1	0	-	0.738	-
2	0.2	0.938	0.917	97.8%
3	0.5	1.238	1.213	98.0%
4	1.0	1.738	1.709	98.3%
5	2.0	2.238	2.206	98.6%

## 4. CONCLUSIONS

In this work, an all-solid-state  $Cl^-$ -ISE with nanowires PEDOT was developed. As the contact layer, the nanowires PEDOT can decrease the charge transfer resistance and increase the redox capacitance. In the range of  $1.0 \times 10^{-4}$  to  $1.0 \times 10^{-1}$  M, the electrode shows an excellent linear feature ( $-58.1 \text{ mV}/\log a_{Cl^-}$ ), and the detection limit is  $1.0 \times 10^{-5}$  M. Furthermore, the chloride ion-selective electrode based on nanowires PEDOT has a good stability of electrode potential, and the nanowires PEDOT is convenient to be synthesized on the surface of GC electrode by galvanostatic electrochemical polymerization method. The all-solid-state  $Cl^-$ -ISE with nanowires PEDOT as solid contact may have a bright future.

## ACKNOWLEDGEMENTS

This work was supported by the National Natural Science Foundation of China (No.61771034).

## References

1. C. Cheng, Z.-M. Huang, W.-Y. Chung, D. G. Pijanowskad, M. Dawgul, *Journal of the Chinese Chemical Society*, 59 (2012) 122.
2. H. S. Toh, C. Batchelor-McAuley, K. Tschulik, R. G. Compton, *The Analyst*, 138 (2013) 4292.
3. M. F. Montemor, J. H. Alves, A. M. Simões, J. C. S. Fernandes, Z. Lourenço, A. J. S. Costa, A. J. Appleton, M. G. S. Ferreira, *Cement and Concrete Composites*, 28 (2006) 233.
4. U. Angst, B. Elsener, C. K. Larsen, Ø. Vennesland, *Cement and Concrete Research*, 39 (2009) 1122.
5. P. Vainikka, D. Bankiewicz, A. Frantsi, J. Silvennoinen, J. Hannula, P. Yrjas, M. Hupa, *Fuel*, 90 (2011) 2055.
6. D. Bankiewicz, P. Vainikka, D. Lindberg, A. Frantsi, J. Silvennoinen, P. Yrjas, M. Hupa, *Fuel*, 94 (2012) 240.
7. M. M. Watt, J. M. Engle, K. C. Fairley, T. E. Robitshek, M. M. Haley, D. W. Johnson, *Org. Biomol. Chem.*, 13 (2015) 4266.
8. T. Riis-Johannessen, K. Severin, *Chemistry - A European Journal*, 16 (2010) 8291.
9. Y. Noguchi, L. Zhang, T. Maruta, T. Yamane, N. Kiba, *Analytica Chimica Acta*, 640 (2009) 106.
10. G. Asimellis, S. Hamilton, A. Giannoudakos, M. Kompitsas, *Spectrochimica Acta Part B: Atomic Spectroscopy*, 60 (2005) 1132.
11. M. Rothmaier, U. Schaller, W. E. Morf, E. Pretsch, *Analytica Chimica Acta*, 327 (1996) 17.
12. P. Sjöberg-Eerola, J. Nylund, J. Bobacka, A. Lewenstam, A. Ivaska, *Sensors and Actuators B: Chemical*, 134 (2008) 878.
13. J.-F. Cheng, J.-C. Chou, T.-P. Sun, S.-K. Hsiung, H.-L. Kao, *Japanese Journal of Applied Physics*, 50 (2011) 037001.
14. J.-C. Chou, G.-C. Ye, D.-G. Wu, C.-C. Chen, *Solid-State Electronics*, 77 (2012) 87.
15. B. Paczosa-Bator, *Talanta*, 93 (2012) 424.
16. J. Li, T. Yin, W. Qin, *Analytica Chimica Acta*, 876 (2015) 49.
17. J. Bobacka, A. Ivaska, A. Lewenstam, *ChemInform*, 39 (2008) 329.
18. L. A. Hussein, N. Magdy, H. Z. Yamani, *Sensors and Actuators B: Chemical*, 247 (2017) 436.
19. Ź. Pławińska, A. Michalska, K. Maksymiuk, *Electrochimica Acta*, 187 (2016) 397.
20. M. R. Abidian, D. H. Kim, D. C. Martin, *Advanced Materials*, 18 (2006) 405.
21. A. K. Cuentas-Gallegos, M. E. Rincón, G. Orozco-Gamboa, *Electrochimica Acta*, 51 (2006) 3794.
22. S.-Y. Zhang, J. Zhang, Y. Liu, X. Ma, H.-Y. Chen, *Electrochimica Acta*, 50 (2005) 4365.
23. Q.-F. Wu, K.-X. He, H.-Y. Mi, X.-G. Zhang, *Materials Chemistry and Physics*, 101 (2007) 367.
24. Y. Li, B. Wang, H. Chen, W. Feng, *Journal of Power Sources*, 195 (2010) 3025.
25. M. Li, Z. Wei, L. Jiang, *Journal of Materials Chemistry*, 18 (2008) 2276.
26. L. Liang, J. Liu, J. C. F. Windisch, G. J. Exarhos, Y. Lin, *Angew. Chem. Int.*, 41 (2002) 3665.
27. S. I. Cho, S. B. Lee, *Account of chemical research*, 41 (2008) 699.
28. Y. Umezawa, K. Umezawa, H. Sato, *Pure & Appl. Chem.*, 67 (1995) 507.
29. P. Sjöberg-Eerola, J. Bobacka, A. Lewenstam, A. Ivaska, *Sensors and Actuators B: Chemical*, 127 (2007) 545.
30. J. Szűcs, T. Lindfors, J. Bobacka, R. E. Gyurcsányi, *Electroanalysis*, 28 (2016) 778.
31. J. Bobacka, *Anal. Chem.*, 71 (1999) 4932.
32. B. Paczosa-Bator, M. Pięć, R. Piech, *Analytical Chemistry*, 87 (2015) 1718.
33. M. Zhou, S. Gan, B. Cai, F. Li, W. Ma, D. Han, L. Niu, *Analytical Chemistry*, 84 (2012) 3480.

34. M. Pięk, R. Piech, B. Paczosa-Bator, *Journal of The Electrochemical Society*, 162 (2015) B257.
35. J. Ping, Y. Wang, J. Wu, Y. Ying, *Electrochemistry Communications*, 13 (2011) 1529.
36. G. Crespo, S. Macho, F. Xavier Rius, *Ion-Selective Electrodes Using Carbon Nanotubes as Ion-to-Electron Transducers*, Vol. 80, 2008.
37. Z. Mousavi, J. Bobacka, A. Lewenstam, A. Ivaska, *Journal of Electroanalytical Chemistry*, 633 (2009) 246.
38. A. Konopka, T. Sokalski, A. Michalska, A. Lewenstam, M. Maj-Zurawska, *Anal. Chem.*, 76 (2004) 6410.

© 2017 The Authors. Published by ESG ([www.electrochemsci.org](http://www.electrochemsci.org)). This article is an open access article distributed under the terms and conditions of the Creative Commons Attribution license (<http://creativecommons.org/licenses/by/4.0/>).